

Synthesis and characterization of a novel fluorene-alt-carbazole polymer to host green, blue, and red phosphorescence

Qinghua Zhao,¹ Yu Bai,¹ Zhuxin Fan,¹ Peipei Wang,¹ Jinjin Li,¹ Dongxu Li,¹ Xinwen Zhang²

¹College of Materials Science and Engineering, Huaqiao University, Xiamen 361021, People's Republic of China

²Key Laboratory for Organic Electronics and Information Displays (KLOEID) and Institute of Advanced Materials (IAM), Nanjing University of Posts and Telecommunications, Nanjing 210023, China

Correspondence to: Q. H. Zhao (E-mail: qhzhao@hqu.edu.cn) and X. W. Zhang (E-mail: iamxwzhang@njupt.edu.cn)

ABSTRACT: A novel fluorene-alt-carbazole polymer host Poly(9,9-dioctyl-9H-fluorene-2,7-diyl-alt-N-tetrahydropyran-3,6-carbazole) (PFCz), composed of *N*-tetrahydropyran-3,6-carbazole and 9,9-dioctyl-2,7-fluorene in the polymer backbone, was synthesized by Suzuki coupling. The PFCz possesses good thermal stability and proper lowest unoccupied molecular orbital (LUMO)/highest occupied molecular orbital (HOMO) energy levels to facilitate the injection and transport of electrons and holes. Upon doping with blue, green, and red phosphors, red - green - blue (R-G-B) phosphorescent devices hosted by PFCz have been fabricated and investigated. In contrast to those of blue and green devices, the red devices give better performances with a maximum luminous efficiency of 4.88 cd/A and a maximum power efficiency of 1.85% at 149.84 cd/m², due to favorable triplet energy level (E_T) of PFCz for red phosphor, bis(2-methyldibenzo[*f,h*]quinoxaline)(acetylacetonate)iridium(III) [Ir(MDQ)₂(acac)]. Additionally, with different doped concentrations of Ir(MDQ)₂(acac), the PFCz-related red devices emit nearly pure red light with Commission Internationale de L'Eclairage (CIE) coordinates of (0.57, 0.38), (0.60, 0.38), (0.61, 0.38), and (0.62, 0.38), which were very close to the standard red (0.66, 0.34) by the National Television System Committee. © 2015 Wiley Periodicals, Inc. *J. Appl. Polym. Sci.* **2016**, *133*, 43234.

KEYWORDS: copolymers; optical properties; properties and characterization

Received 12 August 2015; accepted 17 November 2015

DOI: 10.1002/app.43234

INTRODUCTION

Phosphorescent polymer light emitting diodes (PhPLEDs) have been intensively investigated for their application in high-efficiency, full-color, large-area flat-panel displays, solid-state lighting, and flexible optoelectronics, not only because of 100% internal quantum efficiency in principle by fully utilizing both singlet and triplet excitons,^{1,2} but also their low cost, solution processability, large area fabrication, and mechanical flexibility.³⁻⁹ In general, for an efficient device, phosphorescent emitters are dispersed in a suitable polymer host to reduce its self-quenching and triplet-triplet annihilation at high excitation densities due to long exciton lifetimes and long diffusion lengths.¹⁰ Thus, the choice of a correct polymer host is very challenging as the polymer host should have appropriate energy-level matching with neighboring layers for efficient charge injections, and especially have higher triplet energy level (E_T) than that of the guest for efficient energy transfer from the host to the guest.^{11,12} Furthermore, in order to realize full-color device, R-G-B light should have the balanced device efficiency and good lifetime. However, studies on red PhPLEDs with higher efficiency are still far behind those of green PhPLEDs

due to the lack of red polymer hosts with proper HOMO/LUMO level and high E_T level.

PFs and their derivatives, as typical light-emitting conjugated polymers, have been successful application in red fluorescence PLEDs due to their high photoluminescence (PL) quantum efficiencies, good thermal stabilities, and amenability to functionalization at the 9-position of fluorene.¹³⁻¹⁷ However, they are limited to be used as hosts for phosphorescent PLEDs due to their low E_T of 2.15 eV.¹⁰ Recently, several red-emitting PhPLEDs have been reported that employ PFs and their derivatives as host materials, with iridium or osmium complexes serving as phosphorescent guests.¹⁸⁻²¹ Among them, PFs have been developed by employing substituent at 9-position of fluorene or introducing various comonomers on the polymer backbone. For example, Wu *et al.*¹⁹ reported a fluorene-based polymer PF-TPA-OXD, with electron-withdrawing oxadiazole and electron-donating triphenylamine groups substituted at 9-position of fluorene. The red PhPLEDs using poly{5,5'-[(2,7-9H-fluorene-9,9-diyl)bis(4,1-phenylene)]bis[2-(4-(tert-butyl)phenyl)-1,3,4-oxadiazole]-co-(2,7-9H-fluorene-9,9-diyl)bis[N,N-bis(4-(tert-butyl)phenyl)aniline]-co-9,9-dioctyl-9H-fluorene-2,7-diyl}(PF-TPA-OXD) as a host depicted

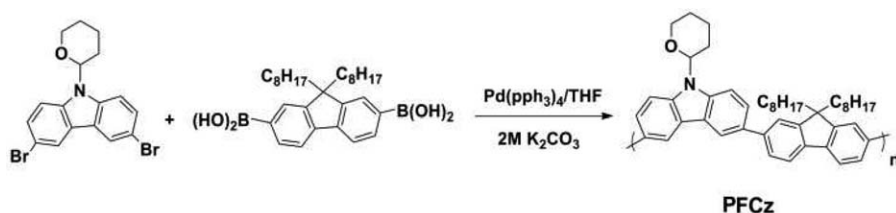


Figure 1. Synthetic procedure of polymer PFCz.

higher maximum external quantum efficiency of 8.37%, while doped with 1 mol % of Os(fppz). Bazan and Moses²⁰ achieved a maximum luminance efficiency of 3 cd/A from red phosphorescent PLEDs with poly(9,9-dihexylfluorene)-co-2,5-dicyanophenylene (PF3CN1) as the host, and 1 wt % tris(2,5-bis-2'-(9',9'-dihexylfluorene)pyridine)iridium(III) (Ir(HFP)₃) as the guest. Chen *et al.*²¹ reported a red host P(tBu-CBPF) with low E_T (2.28 eV), derived from dialkylfluorene and aryl-substituted 3,6-carbazole. Upon doping with 8 wt % red phosphor, it gave a lower maximum luminous efficiency of 2.0 cd/A and a quantum efficiency of 0.75%, due to back energy transfer from red phosphor to host. Significant efforts have been made to develop high efficiency red phosphorescent PLEDs with polyfluorene (PFs) as hosts, but they are scarce and not satisfied with fabrication of full-color flat-panel display.

In this communication, we synthesized a fluorene-alt-carbazole polymer PFCz, composed of *N*-tetrahydropyran-3,6-carbazole and 9,9-dioctyl-2,7-fluorene in the polymer backbone. The obtained PFCz is expected to have higher triplet energy and better hole-transporting ability, owing to high E_T and good hole-transporting ability originating from carbazole units.^{22,23} The photophysical and device properties of PFCz are investigated. The PFCz depicts E_T level of 2.36 eV, slightly higher than that of red phosphorus (2.0 eV). While doped with 6 wt % bis(2-methyl-dibenzo[*f,h*]quinoxaline)(acetylacetonate)iridium(III) [Ir(MDQ)₂(acac)],²⁴ the PFCz-based PhPLEDs show nearly pure red emission with a CIE coordinate of (0.62, 0.38), and this was very close to the standard red (0.66, 0.34) by the National Television System Committee. Moreover, PFCz devices also give a maximum luminous efficiency of 4.88 cd/A and a maximum power efficiency of 1.85% at 149.84 cd/m², which were superior to analogous conjugated polymers with fluorene/carbazole structure.

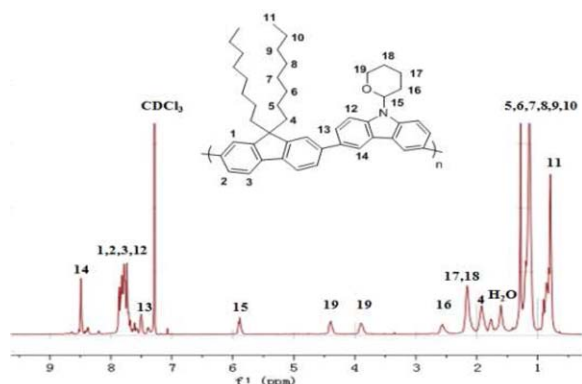


Figure 2. ¹H NMR spectrum of PFCz in CDCl₃. [Color figure can be viewed in the online issue, which is available at wileyonlinelibrary.com.]

EXPERIMENTAL SECTION

Materials and Characterization

N-tetrahydropyran-3,6-dibromo-carbazole was purchased from SunaTech. Tetrakis(triphenylphosphine)palladium(0) (Pd(pph₃)₄) were purchased from Sigma-Aldrich. Tetrahydrofuran (THF) was purified by distillation from sodium in the presence of benzophenone. Other chemicals were used unless otherwise specified.

The ¹H nuclear magnetic resonance (¹H NMR) spectra were recorded with a Varian Mercury Plus 400 spectrometer. The Fourier Transform infrared spectroscopy (FT-IR) spectra were measured on a Shimadzu 8400S spectrometer. The thermal analyses were performed on Shimadzu DTG-60H thermogravimetric analyzer, in a nitrogen atmosphere at a rate of 20°C/min. Differential scanning calorimetry (DSC) was conducted under nitrogen on TA DSC2910/SDT2960. The sample was heated at a temperature of 10°C/min from 30°C to 250°C. UV-vis absorption spectra and PL spectra were measured by Shimadzu UV-3100 spectrophotometer and Edinburgh FL/FS920 TCSPC luminescence spectrophotometer, respectively. Molecular weights and polydispersities of the copolymers were determined by gel permeation chromatography (GPC) analysis, with polystyrene standard calibration (waters high-pressure GPC assembly Model M515 pump, 1-Styragel columns of HR4, HR4E, and HR5E with 500 and 100 Å, refractive index detectors, and solvent THF). Cyclic voltammetry (CV) experiments were carried out with a PARSTAT 2273 electrochemical analyzer, with a three-electrode cell in a solution of Bu₄NBF₄ (0.1 M) in acetonitrile, at a scan rate of 100 mV/s. The polymer films were coated on a square Pt electrode (0.50 cm²) by dipping the electrode into the corresponding solvents and then drying in air. A Pt wire was used as the counter electrode, and an Ag/AgCl (0.1 M) electrode was used as the reference electrode. Prior to each series of measurements, the cell was deoxygenated with nitrogen.

Synthesis

The (9,9-dioctyl-9*H*-fluorene-2,7-diyl)diboronic acid was prepared according to reported procedures.²⁵ Synthesis of P(9,9-dioctyl-2,7-fluorene) was performed following the literature procedure.³

Polymerization of Poly(9,9-dioctyl-9*H*-fluorene-2,7-diyl-alt-*N*-tetrahydropyran-3,6-carbazole) (PCzF). All handling of catalysts and polymerization was performed in a nitrogen atmosphere. To a stirred solution of (9,9-dioctyl-9*H*-fluorene-2,7-diyl)diboronic acid (0.5 g, 1.0 mmol) and *N*-tetrahydropyran-3,6-dibromo-carbazole (0.43 g, 1.0 mmol) in THF, 12 mL of 2 M K₂CO₃ and Pd(pph₃)₄ (0.13 g, 0.1 mmol) were added as the catalyst. After the reaction, solution was refluxed for 24 h, bromobenzene and phenyl boronic acid were added with small

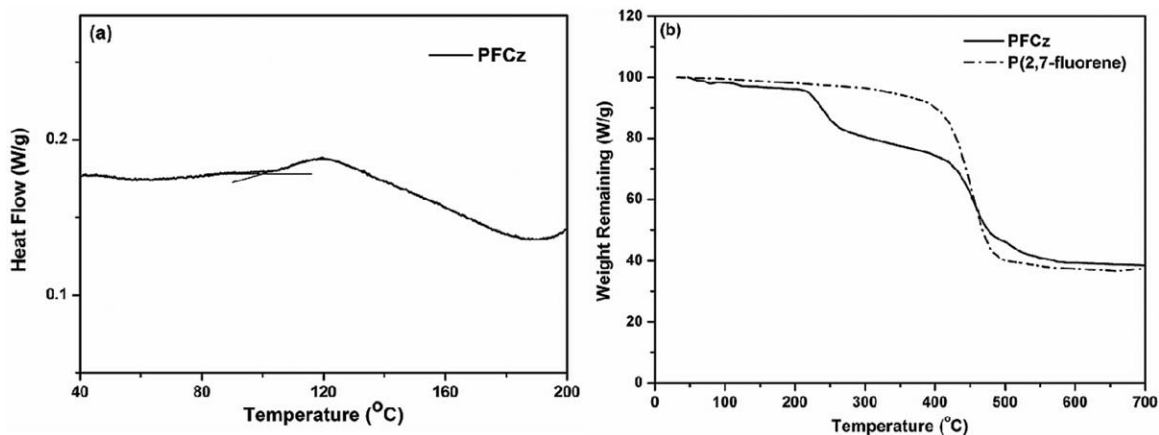


Figure 3. Second heating DSC (a) and TGA (b) spectra of PFCz.

amounts of catalysts for end capping. Then, the reaction was terminated with water, extracted with CHCl_3 , and dried over MgSO_4 . After precipitation was performed twice with chloroform/methanol, the copolymer was obtained. Yield: 0.35 g (56%). ^1H NMR (CDCl_3 , 400 MHz): δ (ppm): 8.61–8.42 (m, 2H, Ar-H), 7.95–7.65 (m, 8H, Ar-H), 7.62–7.32 (m, 2H, Ar-H), 6.0–5.81 (m, 1H, CH), 4.52–4.32 (m, 1H, OCH_2), 3.95–3.72 (m, 1H, OCH_2), 2.62–2.47 (m, 1H, CH_2), 2.32–2.01 (m, 8H, CH_2), 1.98–1.60 (m, 1H, CH_2), 1.35–1.02 (m, 24H, CH_2), 0.95–0.60 (m, 6H, CH_3). Mn: 7.8×10^3 , Mw: 12.1×10^3 , PDI: 1.53 (GPC, PS calibration).

Device Fabrication

An indium-tin oxide (ITO) glass was exposed on oxygen plasma at a power of 50 W and a pressure of 200 mTorr for 5 min. A thin layer (40 nm) of poly(styrene sulfonic acid)-doped poly(ethylenedioxythiophene) (Baytron P CH 8000 from Bayer, its conductivity is 10^{-5} S/cm) was spin-coated on the treated ITO as a hole injection layer. Polymer solutions of host and 1,3-bis[4-tert-butylphenyl]-1,3,4-oxadiazolyl-phenylene (OXD-7) by a 10:4 ratio, and dopant (2–8 wt %) in chlorobenzene (15 mg/mL) were filtered through a 5 μm filter and spin-coated on top of the PEDOT:PSS layer. Then 1,3,5-tris(2-phenylbenzi-

midazolyl)benzene (TPBI) layer (30 nm), which was used as a hole/exciton blocking layer, was grown by thermal evaporation in a vacuum of 2×10^{-6} Torr. At last, a thin layer of LiF (0.5 nm) covered with a layer of aluminum was deposited in a vacuum thermal evaporator through a shadow mask at a vacuum of 2×10^{-6} Torr. The active area of the device was about 10 mm^2 . The red device structures were ITO/PEDOT:PSS (40 nm)/co-host: 2–8 wt % dopant (40 nm)/LiF (0.5 nm)/Al (200 nm). The fabrication of green and blue devices were similar to those of red devices, but device structures were different. The structures of green and blue devices were ITO/PEDOT:PSS (40 nm)/host: 16 wt % dopant (40 nm)/LiF (0.5 nm)/Al (200 nm). The EL spectra and chromaticity coordinates were measured with a SpectraScan PR655 photometer. Current density-voltage-luminance (J-V-L) measurements were conducted simultaneously using a combination of a Keithley source-meter (model 2602) and a calibrated luminance meter. All of the measurements were carried out at room temperature under ambient conditions.

RESULTS AND DISCUSSION

The synthetic procedure for polymer PFCz is outlined in Figure 1. The PFCz was synthesized through a Suzuki coupling reaction. Under the atmosphere of nitrogen, *N*-tetrahydropyran-3,6-

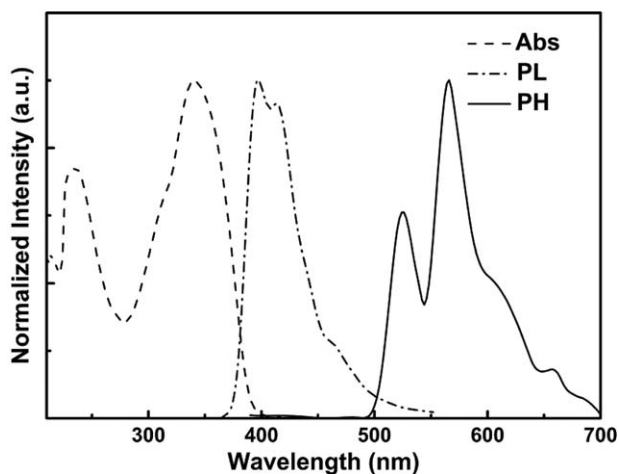


Figure 4. UV-vis, photoluminescent (PL) at 298 K, and phosphorescent spectra (PH) at 77 K in CH_2Cl_2 of PFCz.

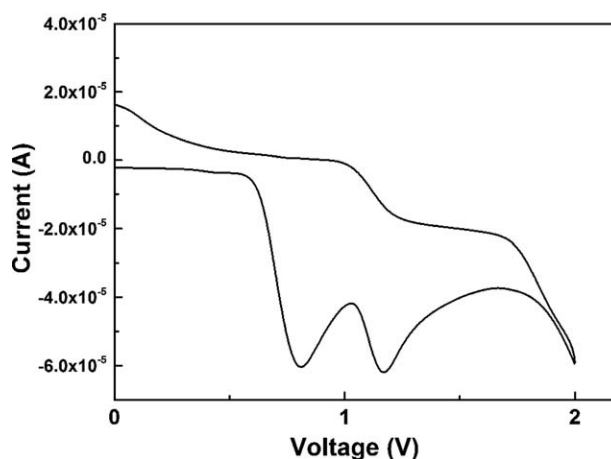


Figure 5. Oxidation cyclic voltammetry curve of PFCz.

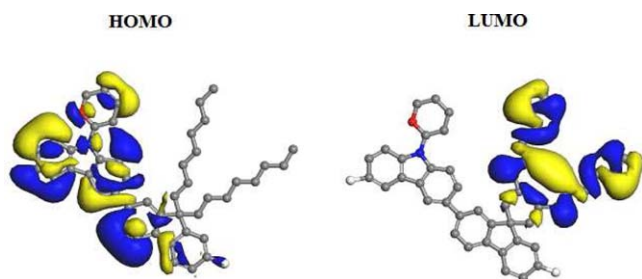


Figure 6. Calculated spatial distributions of the HOMO and LUMO levels of a dimer model of PFCz. [Color figure can be viewed in the online issue, which is available at wileyonlinelibrary.com.]

dibromo-carbazole and (9,9-dioctyl-9H-fluorene-2,7-diyl)diboronic acid were reacted in the case of $\text{Pd}(\text{pph}_3)_4$ and $2\text{M K}_2\text{CO}_3$, and refluxed for 24 h. After the polymerization, the end-capping was accomplished by bromobenzene and phenylboronic acid.

The spectroscopic data of ^1H NMR was well matched with the proposed polymer structure, as shown in Figure 2. The peaks between 7.27 and 8.8 ppm can be assigned to the protons of the aromatic units of PFCz, and the peaks in the range from 0.5 to 2.8 ppm are attributed to its aliphatic protons. The typical peaks at 3.9 and 4.4 ppm are due to resonances of the protons of the alkoxy groups on carbazole units. The polymer PFCz is readily soluble in common organic solvent such as chloroform, THF, and toluene. The weight-average molecular weight (M_w) of PFCz determined by gel permeation chromatography (GPC) using THF as the eluent and polystyrene as standard was 12.1×10^3 with a polydispersity of 1.53.

Thermal Properties

The thermal properties of the polymers were characterized by means of thermogravimetric analysis (TGA) and differential scanning calorimetry (DSC), as depicted in Figure 3. The PFCz shows 5% weight loss around 213°C , which is lower than 350°C of poly(9,9-dioctyl-2,7-fluorene) [Figure 3(b)]. This implies that introduction of carbazole units into the polymer main chain may decrease the thermal stability of the copolymers. A similar phenomenon was also reported for light emitting poly(2,7-fluorene)s with carbazole moiety in the main chain.³ While second heating DSC measurements were performed at a heating scan

rate of $10^\circ\text{C}/\text{min}$ under nitrogen, the PFCz exhibits a glass transition temperature (T_g) about 104°C , and no crystallization or melting behavior in the temperature range 40°C – 200°C , indicating that PFCz has good thermal and morphological stability, which are essential to achieve homogeneous and amorphous thin films upon solution-process for the stable PhPLEDs.

Optical Properties

The UV-visible, fluorescence, and low temperature phosphorescence spectra of the PFCz in dilute solution were shown in Figure 4. The PFCz shows an absorption maximum at 341 nm, and a blue-shift of 51 nm compared with that of PF ($\lambda_{\text{max}} = 392$ nm), which is attributed to interruption of delocalization of π -electrons along the PF backbone by the 3,6-carbazole linkage. For the emission spectra of PFCz, the peaks at 398 nm and 414 nm are related to the nature of polymers with fluorene/carbazole structures.⁴ The optical band gap (3.06 eV) of the polymer was determined from the UV-visible absorption edge (405 nm).²⁶ Furthermore, the low temperature phosphorescence spectra of the PFCz in dilute solution was also measured at 77 K. The value of E_T level of PFCz was estimated from the highest energy 0–0 phosphorescent emission located at 526 nm to be 2.36 eV, which was slightly lower than (2.60 eV) of P(3,6-Cz).²⁰ This is in accordance with studies on polyphenyl molecules,²⁷ PFCz possesses a slightly larger π -electron delocalization over the *p*-terphenyl than *p*-biphenyl conjugation length in P(3,6-Cz), and thus PFCz has lower E_T . On the other hand, the E_T level of PFCz is higher than (2.28 eV) of P(tBu-CBPF), in which PFCz and P(tBu-CBPF) have similar main chains and different side chains.²¹ This display that not only main chains, but also side chains that may also play some role in triplet energies.

Energy Levels of Materials

CV was performed to investigate the electrochemical properties of the polymers. As shown in Figure 5, PFCz exhibits an oxidation wave with an onset potential at about 0.64 eV. The HOMO levels of the polymer are determined from onset potential of first oxidation peak, estimated to be -5.36 eV, calculated from the following formula: $E_{\text{HOMO}} = -(4.72 + E_{\text{OX onset}})$ eV. Combined with the energy gap from the onset of the absorption (3.06 eV), the LUMO energy level of the PFCz is -2.3 eV.

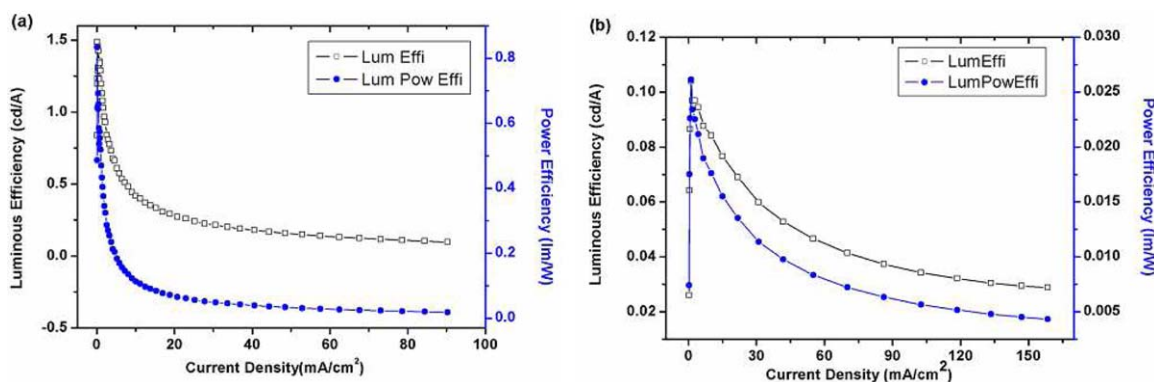


Figure 7. Current density-current density-power efficiency characteristics of the PFCz-based green devices (a) and blue devices (b). [Color figure can be viewed in the online issue, which is available at wileyonlinelibrary.com.]

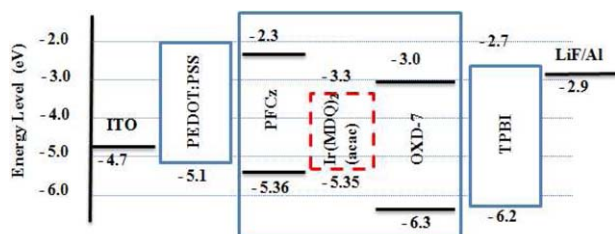


Figure 8. Energy level diagram of the PhPLED containing PFCz host and Ir(MDQ)₂(acac) dopant. [Color figure can be viewed in the online issue, which is available at wileyonlinelibrary.com.]

From the HOMO/LUMO levels, we can observe that HOMO level (−5.36 eV) and LUMO level (−2.3 eV) of PFCz might match well with the work functions of the anode (ITO/PEDOT:PSS: −5.1 eV)²⁸ and the cathode (LiF/Al: −2.9 eV),²⁸ respectively. This suggested that PFCz with suitable HOMO/LUMO levels would be contributed to high efficiency PhPLEDs

using PFCz as a host due to better balance of transport of hole and electron.

Theoretical Calculations

To further understand the structure–property relationship of PFCz at the molecular level, density functional theory (DFT) calculations were performed on a dimer model of PFCz at the B3LYP theoretical level. To the best of our knowledge, calculated spatial distributions of the HOMO and LUMO levels of polymers with fluorene-alt-carbazole structure have not been reported previously. As shown in Figure 6, the HOMO is localized on *N*-tetrahydropyran and polymer backbone, whereas the LUMO is mainly localized on the dioctyl group. The almost complete separation of the HOMO and LUMO will benefit efficient hole- and electron-transporting properties.

EL Performances of Blue, Green, and Red PhPLEDs

To evaluate the ability of PFCz to act as a host for PhPLEDs, we explored PFCz as green and blue host materials and

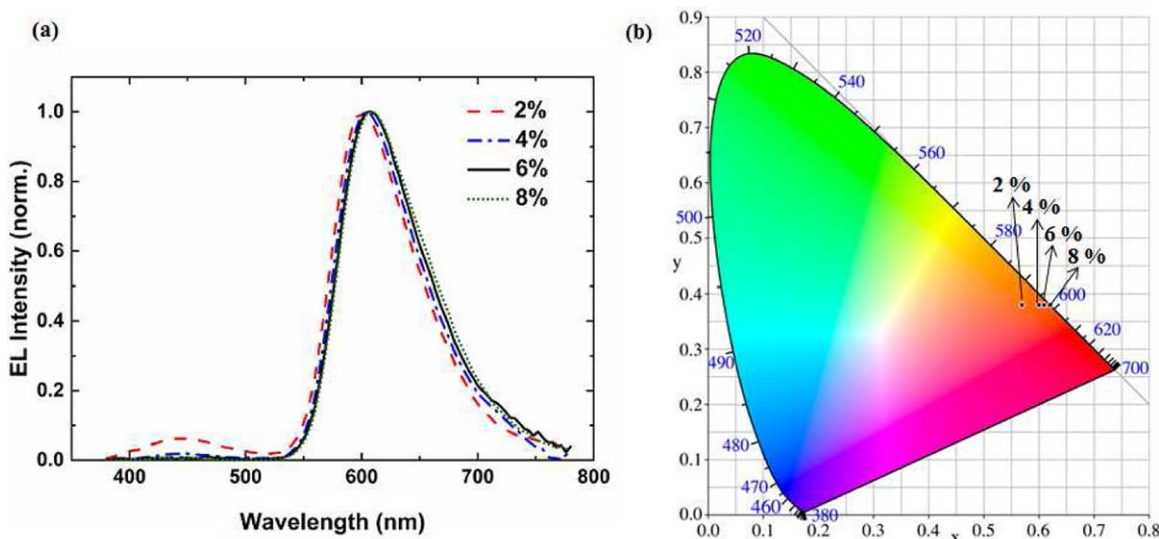


Figure 9. Normalized EL spectra (a) and CIE chromaticity diagram (b) of red PhPLEDs based on PFCz host. [Color figure can be viewed in the online issue, which is available at wileyonlinelibrary.com.]

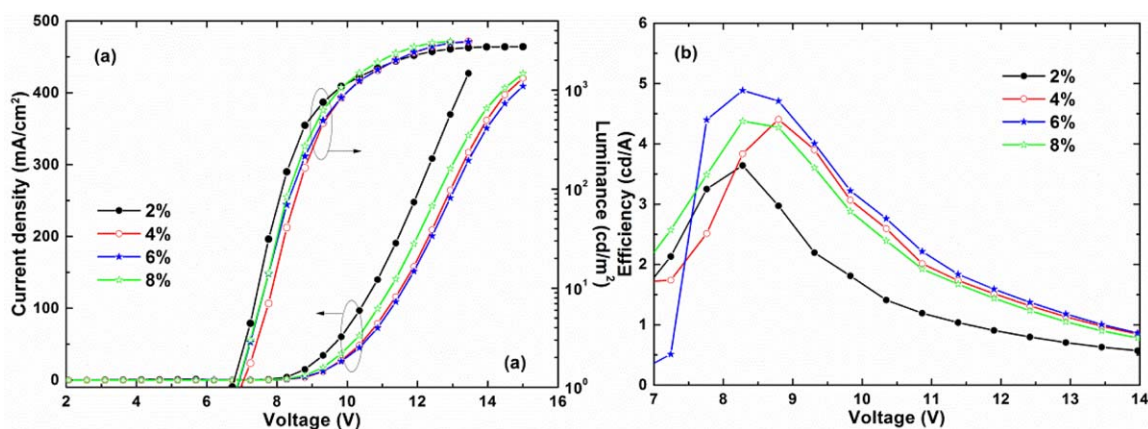


Figure 10. Current density-voltage-luminance (J-V-L) curve (a) and current efficiency-voltage characteristics (b) of the devices based on PFCz. [Color figure can be viewed in the online issue, which is available at wileyonlinelibrary.com.]

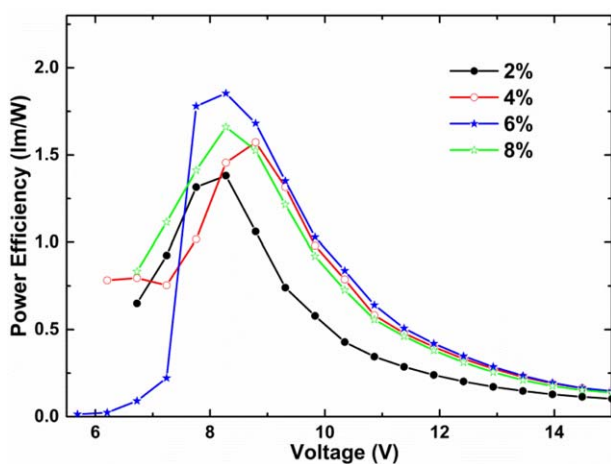


Figure 11. Power efficiency-voltage characteristics of the devices based on PFCz. [Color figure can be viewed in the online issue, which is available at wileyonlinelibrary.com.]

fabricated a single-layer light emitting device with the configuration of ITO/PEDOT:PSS (40 nm)/polymer: 16 wt % dopant (40 nm)/LiF (0.5 nm)/Al (200 nm). The PEDOT:PSS and LiF were served as hole- and electron-injecting layers, respectively. Figure 7 presents current efficiency-current density-power efficiency characteristics of green and blue devices based on PFCz host. While doped with 16 wt % of Irpic (E_T , 2.63 eV), the blue devices gave turn-on voltage of 12 V recorded at 1 cd/m^2 , a maximum luminous efficiency of 0.1 cd/A and a power efficiency of 0.03 lm/W . The green devices doped with $\text{Ir}(\text{ppy})_3$ exhibited turn-on voltage of 3 V recorded at 1 cd/m^2 , a maximum luminous efficiency of 1.06 cd/A , and a power efficiency of 0.66 lm/W . These lower efficiencies in PFCz-based green and blue devices might be due to a back transfer of triplet energy from the dopant to the host.

Because PFCz possesses E_T level of 2.36 eV, higher than that of red phosphor [$\text{Ir}(\text{MDQ})_2(\text{acac})$ (2.0 eV)],²⁴ thus we fabricated double-layer light emitting device with the following configuration: ITO/PEDOT:PSS (40 nm)/EML (60 nm)/TPBI (40 nm)/LiF (0.5 nm)/Al (120 nm). In this architecture, the PEDOT:PSS and LiF served as hole- and electron-injecting layers, respectively; TPBI were used as the hole/exciton-blocking and electron-transporting layer; the emission layer was composed of

Table I. Performances of Red PhPLEDs Using PFCz as a Host

| Polymer | Dopant (wt %) | V_{on}^a [V] | L_{max}^b [cd/m^2] | η_{max}^c [cd/A] | PE^d [lm/W] | CIE [x, y] ^e |
|---------|---------------|-----------------------|---|--|--|-----------------------------|
| PFCz | 2% | 6.7 | 2748 | 3.64 | 1.38 | (0.57, 0.38) |
| | 4% | 7.2 | 3095 | 4.4 | 1.57 | (0.60, 0.38) |
| | 6% | 7.0 | 3073 | 4.88 | 1.85 | (0.61, 0.38) |
| | 8% | 7.1 | 3096 | 4.37 | 1.66 | (0.62, 0.38) |

^aRecorded at 1 cd/m^2 .

^bMaximum luminance.

^cMaximum luminance efficiency.

^dMaximum power efficiency.

^eMeasured at 7 V.

2–8 wt % $\text{Ir}(\text{MDQ})_2(\text{acac})$ as a red guest, PFCz as a host material, and OXD-7 as an electron transporting material with a 10:4 ratio. The energy level diagram of this PhPLEDs is depicted in Figure 8. It is notable that $\text{Ir}(\text{MDQ})_2(\text{acac})$ can act as traps for both electron and hole carriers in PFCz as a host based on their corresponding HOMO and LUMO levels, and PFCz is also served as a triplet blocker to confine the excitons in the emissive layer, due to its E_T of 2.36 eV, higher than 2.00 eV of $\text{Ir}(\text{MDQ})_2(\text{acac})$. Moreover, the hole injection barrier (0.26 eV) from PEDOT:PSS to the PFCz is slightly smaller than the electron injection barrier (0.6 eV) from LiF/Al to the PFCz. Thus, electron-transporting materials OXD-7 and TPBI are used for balancing injection carriers and to further improve device efficiency.

The EL spectra of PFCz-hosted phosphorescent PLEDs at different concentrations of $\text{Ir}(\text{MDQ})_2(\text{acac})$ are depicted in Figure 9(a). There are two distinct emission peaks at 434 nm and at 600 nm, each from the PFCz and $\text{Ir}(\text{MDQ})_2(\text{acac})$, respectively. Upon increasing concentration of $\text{Ir}(\text{MDQ})_2(\text{acac})$ from 2 wt % to 8 wt %, the emission peak from PFCz host gradually reduced and finally disappeared. This implies that an energy transfer from PFCz host to $\text{Ir}(\text{MDQ})_2(\text{acac})$ guest is effective, which is contributed to high efficiency from red phosphorescent PLEDs with PFCz host.

The current density-voltage-luminance (J-V-L), current efficiency-voltage (CE-V), and power efficiency-voltage characteristics of the red PhPLEDs with PFCz host are illustrated in Figures 10 and 11, and the results are summarized in Table I. While varying dopant concentrations of 2, 4, and 6 wt %, the red PhPLEDs depicted the gradually improved device performances. The PFCz devices at 6 wt % doped concentration give a maximum luminous efficiency of 4.88 cd/A and a maximum power efficiency of 1.85 lm/W at 149.84 cd/m^2 . It is regretted that efficiency of red PhPLEDs was a little decreased while increasing $\text{Ir}(\text{MDQ})_2(\text{acac})$ concentration up to 8 wt %, with a maximum luminous efficiency of 4.37 cd/A and a maximum power efficiency of 1.66 lm/W . Though this behavior is far behind the highest efficiency (7.14 cd/A) from Förster Resonance Energy Transfer (FRET)-based hybrid polymers until now,²⁹ this is still superior to those of fluorene-alt-carbazole copolymers with carbazole N-graft cyclometalated Ir complexes.^{30–32} Moreover, as shown in Figure 9(b), while varying $\text{Ir}(\text{MDQ})_2(\text{acac})$ concentration from 2 to 8 wt %, the CIE (1931) coordinates of PFCz devices were determined to be ($X = 0.57, Y = 0.38$), ($X = 0.60, Y = 0.38$), ($X = 0.61, Y = 0.38$), and ($X = 0.62, Y = 0.38$), in which the CIE coordinates were gradually moved toward nearly pure red emission.

CONCLUSIONS

We have synthesized a fluorene-alt-carbazole polymer PFCz, carrying an *N*-tetrahydropyran-substituted carbazole moiety. The PFCz possesses good thermal stability. The calculated spatial distributions of the HOMO and LUMO levels of PFCz show that the HOMO and LUMO levels of PFCz are almost completely separated, which would facilitate the injection and transport of electrons and holes of PFCz. Because of proper E_T level

(2.36 eV) for PFCz, the PFCz-based R-G-B PhPLEDs have been fabricated and investigated, while doped with blue, green, and red phosphors. Among R-G-B devices, the red devices showed best performances. Upon doping with Ir(MDQ)₂(acac) of 6 wt % concentration, the red devices showed a maximum luminous efficiency of 4.88 cd/A and a maximum power efficiency of 1.85 lm/W at 149.84 cd/m². Moreover, the PFCz-related red PhPLEDs were found to emit nearly pure red light with a CIE coordinate of (0.62, 0.38) and this was very close to the standard red (0.66, 0.34) by the National Television System Committee.

ACKNOWLEDGMENTS

This work was financially supported by the National Natural Science Foundation of China (grant no. 51202073, 61204048) and the Startup Package Funding of Huaqiao University (11BS103). Qing-Hua Zhao thanks Promotion Program for Young and Middle-aged Teacher in Science and Technology Research of Huaqiao University (ZQN-PY105) for financial support.

REFERENCES

- Baldo, M. A.; O'Brien, D. F.; You, Y.; Shoustikov, A.; Sibley, S.; Thompson, M. E.; Forrest, S. R. *Nature* **1998**, *395*, 151.
- Wohlgenannt, M.; Tandon, K.; Mazumdar, S.; Ramasesha, S.; Vardeny, Z. V. *Nature* **2001**, *409*, 494.
- Liu, B.; Yu, W. L.; Lai, Y. H.; Huang, W. *Chem. Mater.* **2001**, *13*, 1984.
- Irfan, M.; Belfield, K. D.; Saeed, A. *RSC Adv.* **2015**, *5*, 48760.
- Yin, N. H.; Feng, L. H. *Dyes Pigm.* **2015**, *117*, 116.
- Liang, B. S.; Hu, J.; Liu, Y. P.; Fan, Z. Q.; Wang, X. Y.; Zhu, W. G.; Wu, H. B.; Cao, Y. *Dyes Pigm.* **2013**, *99*, 41.
- Zhao, Q. H.; Kim, Y. H.; Dang, T. T. M.; Shin, D. C.; You, H.; Kwon, S. K. *J. Polym. Sci. Part A: Polym. Chem.* **2007**, *45*, 341.
- Sun, D. M.; Yang, Z. M.; Ren, Z. J.; Li, H. H.; Bryce, M. R.; Ma, D. G.; Yan, S. K. *Polym. Chem.* **2014**, *5*, 220.
- Hu, D. H.; Cheng, G.; Lu, P.; Liu, H.; Shen, F. Z.; Li, F. H.; Lv, Y.; Dong, W. Y.; Ma, Y. G. *Macromol. Rapid. Commun.* **2011**, *32*, 1467.
- Yeh, S. J.; Wu, M. F.; Chen, C. T.; Song, Y. H.; Chi, Y.; Ho, M. H.; Hsu, S. F.; Chen, C. H. *Adv. Mater.* **2005**, *17*, 285.
- Brunner, K.; van, D. A.; Borner, H.; Bastiaansen, J. J. A. M.; Kiggen, N. M. M.; Langeveld, B. M. W. *J. Am. Chem. Soc.* **2004**, *126*, 6035.
- Sudhakar, M.; Djurovich, P.; Hogen-Esch, T.; Thompson, M. E. *J. Am. Chem. Soc.* **2003**, *125*, 7796.
- Lee, B. R.; Lee, W. H.; Nguyen, T. L.; Park, J. S.; Kim, J. S.; Kim, J. Y.; Woo, H. Y.; Song, M. H. *ACS Appl. Mater. Interfaces* **2013**, *5*, 5690.
- Park, M. J.; Lee, J. H.; Jung, I. H.; Park, J. H.; Hwang, D. H.; Shim, H. K. *Macromolecules* **2008**, *41*, 9643.
- Yang, R. Q.; Tian, R. Y.; Yan, J. G.; Zhang, Y.; Hou, Q.; Yang, W.; Zhang, C.; Cao, Y. *Macromolecules* **2005**, *38*, 244.
- Chen, L.; Zhang, B. H.; Cheng, Y. X.; Xie, Z. Y.; Wang, L. X.; Jing, X. B.; Wang, F. S. *Adv. Funct. Mater.* **2010**, *20*, 3143.
- Yeh, H. C.; Chien, C. H.; Shih, P. I.; Yuan, M. C.; Shu, C. F. *Macromolecules* **2008**, *41*, 3801.
- Gong, X.; Ostrowski, J. C.; Bazan, G. C.; Moses, D.; Heeger, A. J.; Liu, M. S.; Jen, A. K. Y. *Adv. Mater.* **2003**, *15*, 45.
- Wu, F. I.; Shih, P. I.; Tseng, Y. H.; Chen, G. Y.; Chien, C. H.; Shu, C. F.; Tung, Y. L.; Chi, Y.; Jen, A. K. Y. *J. Phys. Chem. B* **2005**, *109*, 14000.
- Gong, X.; Ostrowski, J. C.; Bazan, G. C.; Moses, D.; Heeger, A. J.; Liu, M. S.; Jen, A. K.-Y. *Adv. Mater.* **2003**, *15*, 45.
- Chen, Y. C.; Huang, G. S.; Hsiao, C. C.; Chen, S. A. *J. Am. Chem. Soc.* **2006**, *128*, 8549.
- Shao, S. Y.; Ding, J. Q.; Ye, T. L.; Xie, Z. Y.; Wang, L. X.; Jing, X. B.; Wang, F. S. *Adv. Mater.* **2011**, *23*, 3570.
- van, D. A.; Bastiaansen, J. J. A. M.; Kiggen, N. M. M.; Langeveld, B. M. W.; Monkman, R. C.; Brunner, A. K. J. *J. Am. Chem. Soc.* **2004**, *126*, 7718.
- Chang, Y. L.; Wang, Z. B.; Helander, M. G.; Qiu, J.; Puzzo, D. P.; Lu, Z. H. *Org. Electron.* **2012**, *13*, 925.
- Chen, X. W.; Jin, L. L.; Liang, Y. M.; Ahmed, M. O.; Tseng, H. E.; Chen, S. A. *J. Am. Chem. Soc.* **2003**, *125*, 636.
- Kim, S. O.; Zhao, Q. H.; Thangaraju, K.; Kim, J. J.; Kim, Y. H.; Kwon, S. K. *Dyes Pigm.* **2011**, *90*, 139.
- Higuchi, J.; Hayashi, K.; Seki, K.; Yagi, M.; Ishizu, K.; Kohno, M.; Ibuki, E.; Tajima, K. *J. Phys. Chem. A* **2001**, *105*, 6084.
- Fu, Q.; Chen, J. S.; Shi, C. S.; Ma, D. G. *ACS Appl. Mater. Interfaces* **2012**, *4*, 6579.
- Lee, B. R.; Lee, W. H.; Nguyen, T. L.; Park, J. S.; Kim, J. S.; Kim, J. Y.; Woo, H. Y.; Song, M. H. *ACS Appl. Mater. Interfaces* **2015**, *5*, 5690.
- Ying, L.; Zou, J. H.; Yang, W.; Wu, H. B.; Zhang, A. Q.; Wu, Z. L.; Cao, Y. *Macromol. Chem. Phys.* **2009**, *210*, 457.
- Ying, L.; Zou, J. H.; Zhang, A. Q.; Chen, B.; Yang, W.; Cao, Y. *J. Organ. Meta. Chem.* **2009**, *694*, 2727.
- Guo, T.; Guan, R.; Zou, J. H.; Liu, J.; Ying, L.; Yang, W.; Wu, H. B.; Cao, Y. *Polym. Chem.* **2011**, *2*, 2193.